GA–A22911

CONF-980678--

RI–MODE INVESTIGATIONS IN THE DIII–D TOKAMAK WITH NEON AND ARGON INDUCED RADIATING MANTLES

by

G.L. JACKSON, G.M. STAEBLER, M. MURAKAMI, M.R. WADE, J.A. BOEDO,
T.E. EVANS, R.J. LA HAYE, C.J. LASNIER, A.W. LEONARD, G.R. McKEE,
A.M. MESSIAEN, R.A. MOYER, J. ONGENA, T.W. PETRIE, T.S. TAYLOR
B. UNTERBERG, and W.P. WEST

JULY 1998

GENERAL ATOMICS

DISCLAIMER

GA–A22911

RI–MODE INVESTIGATIONS IN THE DIII–D TOKAMAK WITH NEON AND ARGON INDUCED RADIATING MANTLES

by
G.L. JACKSON, G.M. STAEBLER, M. MURAKAMI,[†] M.R. WADE,[†]
J.A. BOEDO,[‡] T.E. EVANS, R.J. LA HAYE, C.J. LASNIER,[◊] A.W. LEONARD,
G.R. McKEE,[△] A.M. MESSIAEN,[§] R.A. MOYER,[‡] J. ONGENA,[§] T.W. PETRIE,
T.S. TAYLOR B. UNTERBERG,[#] and W.P. WEST

This is a preprint of a paper to be presented at the 25th European Physical Society Conference on Controlled Fusion and Plasma Physics, June 29–July 3, 1998, Prague, Czech Republic, and to be published in the *Proceedings.*

[†]Oakridge National Laboratory
[‡]University of California, San Diego
[◊]Lawrence Livermore National Laboratory
[△]University of Wisconsin, Madison
[§]ERM, Brussels, Belgium
[#]KFA, Jüelich, Germany

Work supported by
the U.S. Department of Energy
under Contracts DE-AC03-89ER51114, W-7405-ENG-48,
DE-AC05-96OR22464, and Grant DE-FG03-95ER54294

GA PROJECT 3466
JULY 1998

GENERAL ATOMICS

RI–MODE INVESTIGATIONS IN THE DIII–D TOKAMAK WITH NEON AND ARGON INDUCED RADIATING MANTLES*

G.L. Jackson, G.M. Staebler, M. Murakami,† M.R. Wade,† J.A. Boedo,‡ T.E. Evans,
R.J. La Haye, C.J. Lasnier,Δ A.W. Leonard, G.R. McKee,§ A.M. Messiaen,◊
R.A. Moyer,‡ J. Ongena,◊ T.W. Petrie, T.S. Taylor, B. Unterberg,# and W.P. West
General Atomics, P.O. Box 85608, San Diego, CA 92186-5608

The RI–mode regime, with high radiating power fractions from 0.5 to 0.9, energy confinement enhancements, H_{89P}, over ITER89-P L–mode scaling greater than 1.6, and operation at or above the Greenwald density limit (n_{GW}) is an attractive operating scenario for future fusion burning plasma devices. The TEXTOR tokamak has demonstrated this scenario in a limiter device with steady state conditions, $\Delta t_{RI\text{-}mode}/\tau_E > 100$ [1]. Studies have been initiated on the DIII–D tokamak with the goals of: (a) extending these results to a larger non circular machine (providing size and shape scaling), (b) investigating the underlying physical mechanisms of RI–mode with a complementary diagnostic set to that on TEXTOR, and (c) using non-intrinsic impurities, e.g. neon and argon, to obtain high performance diverted discharges, ($\beta_N H_{89P} > 6$) in support of the DIII–D advanced tokamak (AT) program, where $\beta_N = \beta_T/(I_p/aB_T)$ and β_T, I_p, a, and B_T are toroidal beta (in %), plasma current (MA), minor radius (m), and toroidal magnetic field (T) respectively. We define $P_{radLCFS}$ as the radiated power inside the LCFS and note that nearly all of this radiation occurs in the mantle region $0.6 < \rho < 1.0$, i.e. $P_{mantle} \approx P_{radLCFS}$. Three types of DIII–D discharges where mantle radiation plays a significant role are discussed in this paper: (i) ELMing H–mode "puff and pump," (ii) limiter L–mode, and (iii) high performance.

The first type of discharge with a high fraction of mantle radiation is obtained by puffing deuterium above the midplane into a lower single null shape, where the outer strike point is positioned at the entrance to the DIII–D toroidally continuous cryopump. With argon injection into the divertor region, this technique, termed "Puff and pump" [2], produced ELMing H–mode discharges and under certain conditions there was a significant fraction of radiated power from within the LCFS at high normalized densities, $n_e/n_{GW} <= 0.95$ as shown in Fig. 1. In this discharge, there is a marked increase in the rate of density rise and an increase in the fraction of radiation beginning at 3000 ms, although external parameters are constant, e.g. gas flow, I_p, B_T, q_{95}, P_{NB}, and discharge shape. Both density and confinement continue to increase until the argon puff is terminated at 4000 ms. Energy confinement shown in Fig. 1, f_{H93}, has been normalized to the ITER H93 ELM free confinement scaling relation. Coincident with the decrease in confinement and density, an increase in MHD activity is observed which generally coincides with the end of the density increase in the radiating mantle phase of argon "puff and pump" discharges and in most cases occurs before the termination of the argon puff. This increase in MHD is most likely associated with the onset

---

*Work supported by U.S. Department of Energy under Contracts DE-AC03-89ER51114, DE-AC05-96OR22464, W-7405-ENG-48 and Grant DE-FG03-95ER54294. This work was also done as part of the DIII–D–TEXTOR collaboration supported by DOE and Euratom.

†Oak Ridge National Laboratory.
‡University of California, San Diego.
ΔLawrence Livermore National Laboratory.
§University of Wisconsin, Madison.
◊ERM, Brussels, Belgium.
#KFA, Jüelich, Germany.

of the m/n=3/2 neoclassical tearing mode [3], and further experiments are planned to examine this in more detail.

The temporal behavior of confinement as a function of normalized density is shown in Fig. 2 for #95020 (same as Fig. 1). Similar response has also been observed in TEXTOR [1], although confinement in these ELMing H–mode divertor DIII–D discharges is substantially above the TEXTOR limiter RI–mode scaling, $\tau_E = \tau_{93H} \bullet n_e/n_{GW}$ at the same normalized density, plotted in Fig. 2. After the increase in MHD fluctuations, shown in Fig. 2, the normalized confinement enhancement markedly decreases.

The increase in the rate of density rise in these puff and pump discharges is usually accompanied by increased toroidal rotation, shown in Fig. 3. This radiation increase is similar to the spin-up first observed in VH–mode discharges [4], although the absolute magnitude is lower in these radiating mantle discharges. The MHD activity increases at the time the toroidal velocity begins decreasing, t ≈ 3700 ms.

The puff and pump discharges described here exhibit a heat flux reduction of more than a factor of 2 to the divertor tiles when compared to similar discharges with no impurity radiation. We also note that these ELMing H–mode discharges were not detached. However there is a reduction of the edge pedestal electron pressure as the fraction of mantle radiation increases, shown in Fig. 4.

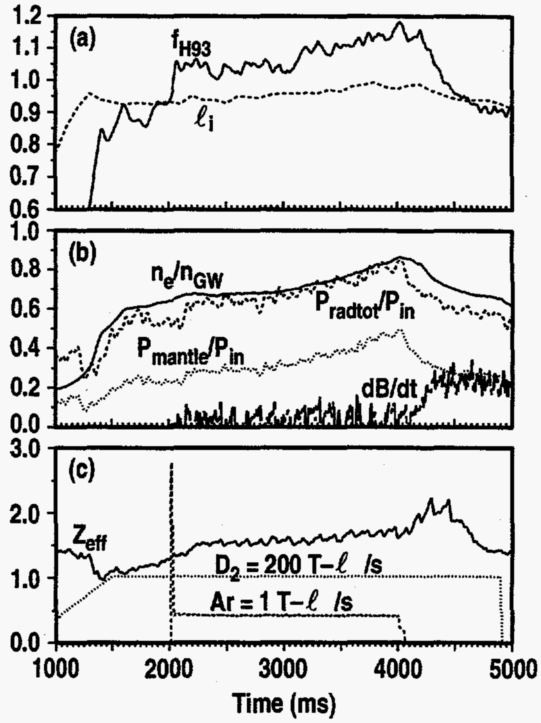

Fig. 1. Temporal evolution of a high density radiating mantle discharge. An increase in the rate of density rise begins at t ≈ 3000 ms. Argon is injected from 2000 to 4000 ms (I_p=1.35MA, B_t = 2.1 T, P_{NB} =6.4-7.3 MW).

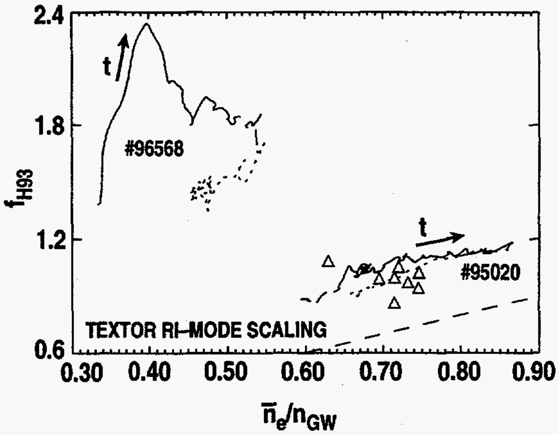

Fig. 2. Normalized confinement as a function of normalized density for the 3 types of discharges: "puff and pump" temporal behavior (#95020), IWL L–mode (points from several discharges), and high performance H–mode (#96568). Solid lines are times during impurity puffing, dashed are before or after, and dots indicate times of significant MHD. The TEXTOR RI–mode scaling relation is also displayed.

Normalized confinement compares favorably with discharges without neon or argon radiation, shown in Fig. 5, where radiating mantle discharges are compared with a subset of the DIII–D ELMing H-mode ITER database with similar parameters (I_p = 1.2–1.4 MA, B_T > 1.65 T, P_{NB} > 3 MW). The addition of non-intrinsic impurities allows an extension to higher density and confinement generally higher than the comparative ITER database discharges. Some of the discharges with neon injection shown in Fig. 5 had transient VH–mode and ELM free phases which generally exhibit higher confinement. The argon puff and pump series were either stationary ELMing

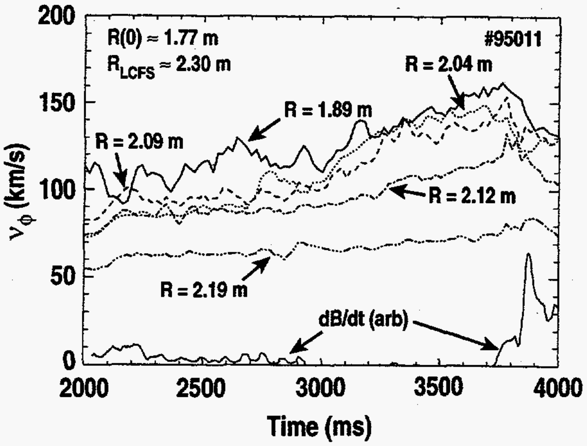

Fig. 3. Toroidal plasma rotation from C^{+6} CER. Discharge conditions are similar to Fig. 1. A "spin up" begins at t=2900 ms. Rotation begins to decrease at approximately the time that MHD activity (also shown) increases, t ≈ 3700–3800 ms.

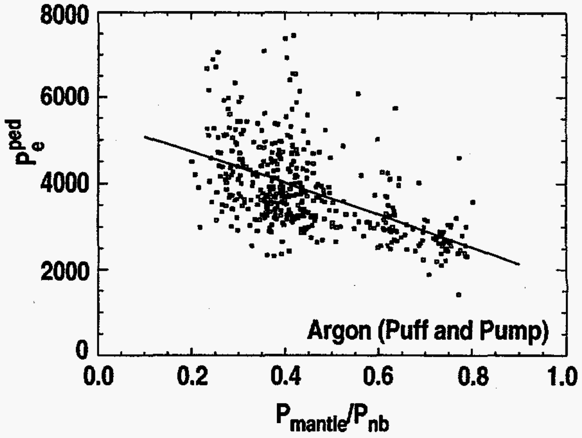

Fig. 4. Edge electron pedestal pressure derived from fits to the H–mode edge pressure profile [8] measured by Thomson scattering. All points are from puff and pump discharges during the time argon was injected. The solid line is a least squares 2nd order polynomial fit to the data.

H–mode, similar to those in the DIII–D ITER database, or slowly evolving ELMing H–mode, such as in Fig. 1.

The second type of DIII–D discharge with a radiating mantle is inner wall limited L–mode. Neon was injected (above the midplane) into L–mode inner wall limited (IWL) discharges (I_p =1.2–1.4 MA, B_T = 1.7-2.1T, q_{95} = 2.8–3.8, P_{NB} = 6–9 MW). Due to technical constraints, operation on the DIII–D outer bumper poloidal limiters is severely limited so the TEXTOR configuration could not be reproduced exactly (TEXTOR RI–mode discharges are limited on the ALTII pumped limiter located below the outer midplane). Nevertheless, this series of DIII–D discharges had features similar to the TEXTOR RI–mode [5]. To date, MARFing has limited the maximum density achieved in DIII–D L–mode IWL discharges to $n_e/n_{GW} \leqq$ 0.75 which is the lower normalized density range observed by TEXTOR. This is probably a consequence of the differences in the limiting surfaces between the two machines. As shown in Fig. 2, confinement at the same normalized density is higher than the TEXTOR scaling relation plotted in Fig. 2. We also note that long duration L–mode IWL discharges without MARFing have not yet been demonstrated in DIII–D.

The third type of discharge where mantle radiation can be important is high performance H– and VH–mode discharges. Impurity seeding has been used to obtain high performance discharges with $\beta_N H > 10$ for 0.55 s and $\beta_N H > 6$ for 1.6 s (#96568). In the latter case, operation at the DIII–D empirical stability limit [6], $\beta_N \approx 4\ell_i$ was maintained for 1.4 s, where ℓ_i is the normalized internal plasma inductance. Neon injection has also allowed VH–mode at the highest target density ever achieved, 6×10^{19} (#93450), nearly a factor of 2 higher than the normal target density for the L to H transition and VH–mode confinement [5].

Mantle radiation in these high performance discharges is substantially lower than the discharges described previously. For example, in the two discharges mentioned above, the fraction of mantle radiation was $\lesssim$ 0.25. However, this is still substantially higher than standard VH–mode discharges, where $P_{mantle}/P_{in} < 0.1$. Although $Z_{eff}(0)$ is low in these discharges, < 2, higher impurity concentrations are observed in the mantle region. This increase in Z_{eff} can provide a stabilizing effect for electron temperature gradient (ETG) modes, allowing increases in particle and energy confinement. Such suppression has been observed in some DIII–D discharges with neon puffing [7].

In conclusion, non-intrinsic impurities have been used in DIII–D to simultaneously obtain good confinement ($\tau_E/\tau_{ITER\text{-}93H} > 1$), high density ($n_e/n_{GW} > 0.8$), significant mantle radiation ($P_{rad}/P_{in} > 0.4$), and reductions in peak heat flux to the walls of more than a factor of 2. L–mode limiter discharges have been obtained under similar conditions, but at lower normalized density. In addition, discharges with $\beta_N H$ of greater than 6 have been observed with impurity radiation. We have focused in this paper on the role of impurities inside the separatrix flux surface. Radiating divertor discharges have also been achieved in DIII–D and have been reported elsewhere [2].

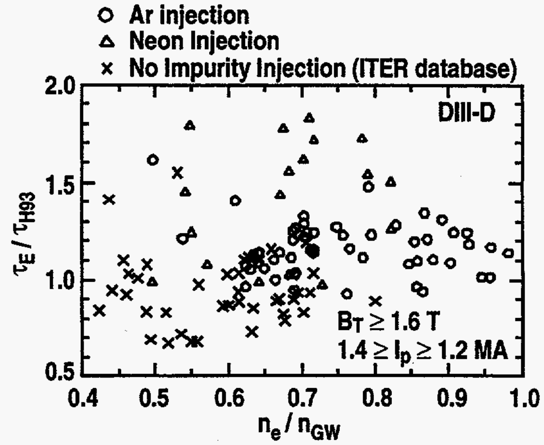

Fig. 5. A comparison of confinement with impurity puffing to ELMing H–mode discharges from the DIII–D ITER database discharges.

The role of increased toroidal rotation in the argon puff and pump experiments can contribute to enhanced confinement, similar to the VH–mode. The increased rotation has also been observed in some DIII–D L–mode IWL discharges such as those discussed in this paper. Whether this “spinup” is a fundamental characteristic of the TEXTOR RI–mode and radiating mantle DIII–D discharges is currently under investigation. The plasma rotation may also be important in maintaining a low central Z_{eff}. For example, impurity concentrations in the argon puff and pump experiments were sufficiently low that $Z_{eff} \lesssim 2$ during the phase of increasing density. However the onset of the m/n=3/2 MHD activity and a decrease in rotation shown in Fig. 3 is accompanied by a rapid increase in Z_{eff}.

Future work will focus upon obtaining stationary radiating mantle discharges, identifying the underlying physical mechanisms, and determining the feasibility and advantages of employing radiating mantle operation in future fusion burning plasma devices such as ITER.

References

[1] J. Ongena, *et. al.* these proceedings (1998).

[2] M.R. Wade, J.T. Hogan, S.L. Allen, *et. al.*, 13th Conf. on Plasma Surface Inter. in Control. Fus. Dev., San Diego, CA, USA (1998), to be published in J. Nuc. Mater.

[3] R.J. La Haye, J.D. Callen, M.S. Chu, *et. al.*, Proc. of 16th Int Conf on Fus Energy IAEA Montreal 7-11 October 1996, Vol 1, p 747 , Vienna 1997.

[4] G.L. Jackson, J. Winter, T.S. Taylor, *et. al*, Phys. Fluids B **4** (1992) 2181.

[5] G.L. Jackson, M. Murakami, G.M. Staebler, *et. al.*, 13th Conf. on Plasma Surface Inter. in Control. Fus. Dev., San Diego, CA, USA (1998), to be published in J. Nuc. Mater.

[6] E.J. Strait, “Stability of High Beta Tokamak Plasmas,” Phys. Plasmas **1** (1994) 1415.

[7] G.M. Staebler, G.L. Jackson, W.P. West, *et. al*, submitted to Phys. Rev. Lett. (1998).

[8] R.J. Groebner and T.H. Osborne, Phys. Plasmas **5** (1998) 1800.